

Bending instabilities in magnetized accretion discs

Vasso Agapitou^{1*}, John C. B. Papaloizou¹ and Caroline Terquem^{2,1,3}

¹ *Astronomy Unit, School of Mathematical Sciences, Queen Mary & Westfield College, Mile End Road, London E1 4NS, UK*

² *Lick Observatory, University of California, Santa Cruz, CA 95064, USA*

³ *Laboratoire d'Astrophysique, Université Joseph Fourier/CNRS, BP 53, 38041 Grenoble Cedex 9, France*

Received; Accepted

ABSTRACT

We study the global bending modes of a thin annular disc subject to both an internally generated magnetic field and a magnetic field due to a dipole embedded in the central star with axis aligned with the disc rotation axis. When there is a significant inner region of the disc corotating with the star, we find spectra of unstable bending modes. These may lead to elevation of the disc above the original symmetry plane facilitating accretion along the magnetospheric field lines. The resulting non-axisymmetric disc configuration may result in the creation of hot spots on the stellar surface and the periodic photometric variations observed in many classical T Tauri stars (CTTS). Time-dependent behaviour may occur including the shadowing of the central source in magnetic accretors even when the dipole and rotation axes are aligned.

Key words: accretion, accretion discs – MHD – instabilities – stars: magnetic fields.

1 INTRODUCTION

Situations in which a thin accretion disc is threaded by a strong poloidal magnetic field are of interest in different astrophysical contexts relating to accreting objects such as neutron stars or young stellar objects. This situation may result when the disc interacts with a magnetic field produced by a dipole embedded in the central star such that the dipole field lines penetrate the disc (Ghosh & Lamb 1978, Ghosh & Lamb 1979, Campbell 1987, Camenzind 1990, Königl 1991).

In addition open poloidal field lines may be advected inwards by the accreting matter (Lubow, Papaloizou & Pringle 1994, Reyez-Ruiz & Stepinski 1996, Agapitou & Papaloizou 1996) and be associated with a centrifugally driven wind (see Königl 1993 for a review). The observed correlation between mass accretion rate and mass outflow rate in T Tauri stars (TTS) supports the idea of the accretion disc as the underlying source of the outflows emanating from young stars (Cabrit et al. 1990).

The short-term photometric variability evident in many CTTS has been attributed to the presence of both dark and hot spots that cover a part of the stellar surface (Bouvier 1994, Bouvier et al. 1995). The latter have been explained as arising from shocks formed close to the stellar surface resulting from non-axisymmetric accretion along stellar magnetic field lines. Such magnetospheric accretion is also invoked to explain the large infall velocities inferred from emission lines (Calvet & Hartmann 1992, Edwards et al. 1994, Hartmann, Hewett & Calvet 1994), the infrared colours of TTS (Kenyon, Yi & Hartmann 1996) and the outbursts of EX Lupi (Lehmann, Reipurth & Brandner 1995). Most of the variability of TTS cannot be accounted for unless there is some time-dependence in the magnetic field and(or) the accretion flow (Bouvier et al. 1995). The presence of an accretion disc around many TTS seems also to be linked to their low rotational velocities and the kind of activity observed on the stellar surface (Edwards et al. 1993, Montmerle et al. 1993).

Under some conditions, the interaction of a strong stellar dipole field with a surrounding low mass disc prevents accretion. This is because the magnetic stresses exerted on the disc, external to the radius where the star corotates with the local disc material which has near-Keplerian rotation, act so as to transfer angular momentum to the disc and spin down the star. The accretion disc is then truncated at a radius where the viscous and magnetic torques balance. Models of this type have been developed to account for the low rotational velocities of TTS provided that the accretion disc is not dissipated too early in

* V.Agapitou@qmw.ac.uk

the star's lifetime (Cameron & Campbell 1993, Yi 1994, Ghosh 1995, Armitage & Clarke 1996). We note though that non-magnetized stars could also experience spin-down while they accrete mass. Paczynski (1991) and Popham & Narayan (1991) have shown that when a star rotates close to its breakup speed the accreted specific angular momentum decreases and it even attains negative values for large enough values of the stellar rotation speed.

The situation of no or low mass accretion together with stellar spin down occurs when the field is strong and the disc mass is low giving rise to a small viscous angular momentum flux. In this paper we shall consider the converse situation when the disc is massive enough to penetrate through to the corotation region so that accretion becomes possible. As in previous studies, we assume the existence of a dipole field embedded in the central star. The present observational evidence cannot rule out such a coherent field structure (Montmerle et al. 1994). There is evidence from numerical calculation of non-linear stellar dynamos that a steady dipole mode is the most easily excited one (Brandenburg, Tuominen & Moss 1989). The possibility of a fossil field has also been proposed (Tayler 1987).

In this paper we adopt the model of Spruit & Taam (1990) which is such that when the disc is able to reach interior to the corotation radius, the inner parts which contain field lines connected to the central star, corotate with it. In that case, simple thin disc models in which the magnetic field plays an important part in supporting the inner corotating region against gravity can be constructed when the axis of the dipole and the disc angular momentum axis are aligned (Spruit & Taam 1990, 1993). Considering the inner corotating disc to be part of the magnetosphere, these models have the fastness parameter, or ratio of stellar to inner differentially rotating disc angular velocity, close to unity. Magnetic support may also be important in the outer, differentially rotating part of the disc if an inwardly advected field becomes strong, as would be the case in the presence of a strong wind removing most of the disc angular momentum (see for example Königl 1989).

The importance of the issue of the stability of these disc models has been stressed by Spruit & Taam (1990) who considered the role of interchange instabilities in enabling matter to migrate inwards in the inner corotating region of the disc until direct particle motion confined to equilibrium vacuum field lines becomes possible. However, note that such particle motion along vacuum field lines may not be representative of the plasma flow that may occur along field lines because the plasma may in principle contain significant currents that disturb the original vacuum field lines. A study of the possible flow along field lines accordingly requires a full MHD treatment. The local stability of the outer differentially rotating disc to interchange modes has been considered by Spruit, Stehle & Papaloizou (1995).

In this paper, we study the global stability of a thin magnetized accretion disc to both axisymmetric and non-axisymmetric disturbances perpendicular to its plane (bending modes). These are the thin disc limit of modes with density perturbation having odd symmetry with respect to reflection in the mid-plane, in contrast to the interchange modes which have even symmetry. At equilibrium the disc is permeated by both an internally produced poloidal magnetic field and an external dipole field. We here limit consideration to the case when the vertical component of the field in the inner disc does not change sign. Bending modes are of potential interest because an instability may lead to elevation of the disc mid-plane above the original symmetry plane leading to facilitated motion along field lines connected to the star as well as time-dependent shadowing of the central source. In the context of neutron stars this was also pointed out by Spruit & Taam (1990). The accretion along magnetic field lines derived from a non-axisymmetric disc would result in the production of hot spots on the stellar surface and modulation of the power output. This could lead to a time-dependent accretion flow even in the aligned dipole case and it may account for the irregular variability of CTTS without the need to invoke a variable magnetic field. Finally, non-axisymmetric modes with azimuthal mode number $m = 1$ are related to disc precession (Papaloizou & Terquem 1995) and are of potential interest with regard to precessing jets.

In section 2 we describe the thin equilibrium disc models. In section 3 we give the perturbation equations for linear modes under the *ab initio* assumption of a razor-thin disc. We derive the local dispersion relation which indicates instability in the inner corotating parts of the disc if they are extensive enough. We further derive variational principles for the axisymmetric modes showing that the unstable modes do occur in discs with finite albeit small thickness. We give a simple physical picture of the instability showing how it originates as an unstable interaction between the central dipole and current loops in the disc. In section 4 we describe the specific equilibrium disc models that we consider and our numerical calculations. They give spectra of axisymmetric and non-axisymmetric unstable modes confined to the disc inner regions. These results are presented in section 5. Finally in section 6 we discuss possible consequences of our results.

2 EQUILIBRIUM DISCS

We consider thin disc configurations with an axisymmetric poloidal magnetic field $\mathbf{B} = (B_r, 0, B_z)$. Here we use cylindrical polar coordinates (r, ϕ, z) . The field is described by a flux function ψ such that

$$B_r = \frac{-1}{r} \frac{\partial \psi}{\partial z} \text{ and } B_z = \frac{1}{r} \frac{\partial \psi}{\partial r}. \quad (1)$$

For this field the current density $\mathbf{j} = (0, j_\phi, 0)$. For an infinitesimally thin disc it is convenient to work with the vertically integrated azimuthal component of the current density J , where

$$J = \int_{-\infty}^{\infty} j_{\varphi} dz.$$

By integrating the azimuthal component of Ampère's law through the disc, we obtain

$$B_r^+ = J/2, \quad (2)$$

where B_r^+ denotes the radial component of the magnetic field on the upper surface of the disc. Here we have set the magnetic permeability, μ_0 , to unity. We can recover the equations in MKSA units by replacing B by $B/\sqrt{\mu_0}$ and J by $J/\sqrt{\mu_0}$. B_r is antisymmetric with respect to reflection in the disc mid-plane so that its value on the lower surface of the disc is $B_r^- = -B_r^+$. Thus B_r changes significantly on passing through the disc in contrast to B_z which, as implied by the condition $\nabla \cdot \mathbf{B} = 0$, changes negligibly on passing through an infinitesimally thin disc.

2.1 Force balance

The vertical integration of the radial component of the momentum equation yields the condition for radial equilibrium as

$$\Sigma \frac{\partial \Phi}{\partial r} = \Sigma r \Omega^2 + J B_z, \quad (3)$$

where Σ is the surface density, Ω is the disc angular velocity, and Φ is the gravitational potential.

The above formalism neglects the radial pressure force. An infinitesimally thin disc can in practice be considered to be significantly thinner than c_s/Ω (c_s being the sound speed). The vertical equilibrium then implies that the mid-plane pressure $P \sim (B_r^+)^2$, since the magnetic squeezing of the disc overwhelms its tidal confinement. Thin disc equilibrium configurations of strongly magnetized discs with the above properties, which take account of the vertical structure, have been constructed by Ogilvie (1997). In order to neglect pressure forces in the radial direction, we require, assuming $B_r^+ \sim B_z$, that $H \ll L_r$, where H is the semi-thickness of the disc, and L_r is the scale length of variation in the radial direction. Thus the approximation scheme becomes better for thinner discs. We consider equilibria for which the gravity is due to a central point mass, M , such that

$$\Phi = -\frac{GM}{\sqrt{r^2 + z^2}}.$$

Equilibrium models may be constructed with the surface density, Σ , and integrated current density, J , being specified as arbitrary functions of r . The flux function with no external sources is then given by (see Lubow et al. 1994)

$$\psi(r, z) = \frac{r}{4\pi} \int_{R_i}^{R_o} \int_0^{2\pi} \frac{J(r') \cos(\varphi') r' d\varphi' dr'}{\sqrt{r^2 + r'^2 - 2rr' \cos(\varphi') + z^2}}, \quad (4)$$

where the disc is presumed to have inner and outer boundary radii R_i and R_o respectively, the latter possibly being infinite. To the above internally produced flux, we may add a contribution due to external sources, ψ_{ext} . When the external source is a dipole at the origin,

$$\psi_{\text{ext}} = -B_z^{\text{ext}}(R_i) \frac{R_i^3 r^2}{(r^2 + z^2)^{3/2}}, \quad (5)$$

where $B_z^{\text{ext}}(R_i)$ is the external vertical field at the disc inner boundary.

In the presence of a central dipole, some of the field lines which cross the inner regions of the disc may join to the dipole in the centre. Further out, field lines may be open in the case of an infinite disc or close before the outer boundary when the disc is finite. Field lines with these properties appropriate to an equilibrium configuration are illustrated in Fig. 2 below. The sign of the azimuthal current density in this and all other configurations we consider here is such that the sign of the vertical field in the inner regions of the disc does not change. That is there is no X point. This is the situation naturally expected if dipole field lines diffuse into the disc.

For physical consistency, field lines joining the central dipole should be in a state of isorotation at constant angular velocity, so Σ should be specified accordingly (see section 4.3). The condition of isorotation means that the magnetic field must make an increasingly important contribution to support the fluid against gravity as r decreases. Spruit & Taam (1990) have argued that material moving inwards from the outer disc due to angular momentum transport processes occurring in accretion discs (see Papaloizou & Lin 1995 for a review) can migrate inwards into the isorotating region due to the action of interchange instabilities. This may produce a magnetically dominated isorotating thin disc if the material remains cool. In fact in order to establish an inner corotating part of the disc, magnetic support against gravity should not be large at the outer corotation radius. Assuming $B_r^+ \sim B_z$, this requirement gives at that radius

$$B_z^2 \ll \frac{\Sigma GM}{r^2}.$$

Using $\dot{M} = 2\pi r v_r \Sigma$, v_r being the radial velocity, and the viscous inflow rate $v_r = -\nu/r$, ν being the kinematic viscosity, we obtain

$$B_z^2 \ll \frac{GM|\dot{M}|}{2\pi\nu r^2}.$$

Thus, as indicated above, for fixed stellar properties and disc viscosity, establishment of an inner corotating region is favoured at large accretion rates, $|\dot{M}|$, and accordingly large disc masses.

Open field lines in the outer disc may in principle rotate at any angular velocity. Field lines that close in the outer regions of a finite disc may be opened if there are additional external currents which could be produced by, for example, a wind.

3 PERTURBATION EQUATIONS

We consider linear perturbations of the equilibrium configurations with a Lagrangian displacement ξ which, for a razor-thin disc, has the form

$$\xi = (0, 0, \xi_z).$$

The only non-negligible component is the vertical one which is independent of z . This displacement belongs to a class such that ξ_z is even, while the other components are odd with respect to reflection in the disc mid-plane. These are thus bending modes. We may also assume that the φ -dependence of the perturbations is through a factor $\exp(im\varphi)$, m denoting the azimuthal mode number. From now on this factor will be taken as read and will be dropped from the perturbations. The Eulerian perturbations of the various quantities are denoted by a prime.

The perturbation of the magnetic field interior to the disc, \mathbf{B}' , is related to ξ by the integration of the linearized induction equation with respect to time

$$\mathbf{B}' = (B'_r, B'_\varphi, B'_z) = \nabla \times (\xi \times \mathbf{B}) \quad (6)$$

The non-zero components of \mathbf{B}' take the form

$$B'_r = -\xi_z \frac{\partial B_r}{\partial z}, \text{ and } B'_z = \frac{1}{r} \frac{\partial(r B_r \xi_z)}{\partial r} \quad (7)$$

where B'_z is antisymmetric with respect to reflection in the disc mid-plane and B'_r is symmetric.

The vertical component of the perturbed field in the disc must be matched to the vertical component of the perturbed vacuum field exterior to the disc. The perturbed vacuum field may be taken to be a potential field. This is the case even when the disc takes the form of an annulus making the vacuum multiply connected, because the symmetry properties of the magnetic field perturbation make it circulation-free. On the upper disc surface we therefore have $\partial\Phi'_M/\partial z = B_z'^+$, where $B_z'^+$ is the value of the vertical field perturbation just outside the disc surface and Φ'_M is the magnetic potential associated with the external field perturbation. Continuity of the vertical field component at the upper disc surface implies that Φ'_M can be found using (7). Thus we obtain that on the upper surface

$$\frac{\partial\Phi'_M}{\partial z} = \frac{1}{r} \frac{\partial(r B_r^+ \xi_z)}{\partial r}. \quad (8)$$

The corresponding equation with $+ \rightarrow -$ applies on the lower surface. Finding Φ'_M is entirely analogous to finding the gravitational potential Ψ due to a disc surface density distribution (see Tagger et al. 1990, Spruit et al. 1995). If Φ'_M is taken to be equivalent to Ψ , the appropriate surface density is equivalent to $B_z'^+/(2\pi G)$, where G is the gravitational constant. Thus Φ'_M may be written in the form of a Poisson integral

$$\Phi'_M = -\frac{1}{2\pi} \int_{R_i}^{R_o} \int_0^{2\pi} \frac{B_z'^+(r') \cos(m\varphi') r' dr' d\varphi'}{\sqrt{r'^2 + r^2 - 2rr' \cos(\varphi') + z^2}}. \quad (9)$$

The radial component of the magnetic field perturbation on either the upper or lower surfaces of the disc, just outside the disc, is then given by

$$B_r'^+ = B_r'^- = \left(\frac{\partial\Phi'_M}{\partial r} \right)_{z=0}. \quad (10)$$

3.1 Vertical component of the equation of motion

In general, the vertical component of the Lorentz force per unit volume is

$$F_z = -\frac{1}{2} \frac{\partial B_r^2}{\partial z} + B_r \frac{\partial B_z}{\partial r}. \quad (11)$$

Perturbing and integrating this vertically through the disc gives

$$\int_{-\infty}^{\infty} F'_z dz = -2B_r^+ B_r'^+ - 2\xi_z B_r^+ \frac{\partial B_z}{\partial r} \quad (12)$$

where we have assumed that B_z is almost independent of z in the disc. The perturbed vertically integrated z -component of the equation of motion is

$$\Sigma \frac{D^2 \xi_z}{Dt^2} = -\Sigma \left(\frac{\partial^2 \Phi}{\partial z^2} \right)_{z=0} \xi_z + \int_{-\infty}^{\infty} F'_z dz \quad (13)$$

where D denotes the convective derivative.

The coefficients of equation (13) are independent of t . We can therefore look for solutions in the form of normal modes. In this case the time-dependence of the perturbed quantities is taken to be through a factor $\exp(i\sigma t)$, where σ is the eigenfrequency of the mode. Using this together with the fact that for a point mass potential

$$\left(\frac{\partial^2 \Phi}{\partial z^2} \right)_{z=0} = GM/r^3 = \Omega_K^2,$$

where Ω_K is the keplerian angular velocity, equation (13) becomes the normal mode equation

$$\left[(\sigma + m\Omega)^2 - \Omega_K^2 - \frac{2B_r^+}{\Sigma} \frac{\partial B_z}{\partial r} \right] \xi_z = \frac{2B_r^+}{\Sigma} \left(\frac{\partial \Phi'_M}{\partial r} \right)_{z=0}. \quad (14)$$

Equation (14) together with (9) and (7) constitutes a linear eigenvalue problem with σ as the eigenvalue and ξ_z as the eigenfunction.

3.2 Local Dispersion Relation

We can derive a local dispersion relation from (14) by adopting perturbations of the form $\xi_z \propto \exp(ikr)$, where k is the radial wavenumber, assumed to be $\gg |m|/r$. We comment that because the evaluation of Φ'_M is equivalent to calculation of the gravitational potential due to a surface density $B_z^+/(2\pi G)$, the situation here is closely analogous to that for bending modes in a self-gravitating disk (see Hunter & Toomre 1969, Shu 1984). The integral in (9) can thus be calculated using the WKB approximation to give

$$\Phi'_M = -B'_z/|k| = -ikB_r^+ \xi_z/|k|$$

where Φ'_M is now the amplitude of the mode with radial wavenumber k . The local dispersion relation derived from (14) is then

$$(\sigma + m\Omega)^2 = \Omega_K^2 + \frac{2B_r^+}{\Sigma} \frac{\partial B_z}{\partial r} + \frac{2(B_r^+)^2}{\Sigma} |k|. \quad (15)$$

Instability ensues on the existence of at least one mode with growth rate $i(\sigma + m\Omega) > 0$, for which we require $(\sigma + m\Omega)^2 < 0$. As the last term on the right-hand side of (15) is positive definite and therefore stabilising, the condition for instability becomes

$$\Omega_K^2 + \frac{2B_r^+}{\Sigma} \frac{\partial B_z}{\partial r} < 0. \quad (16)$$

When the gravity is due to a central point mass, (3) gives

$$r(\Omega_K^2 - \Omega^2) = \frac{2B_r^+ B_z}{\Sigma}, \quad (17)$$

so that (16) may be expressed in the equivalent form

$$\frac{\Omega_K^2}{(\Omega_K^2 - \Omega^2)} + \frac{r}{B_z} \frac{\partial B_z}{\partial r} < 0. \quad (18)$$

We comment that in the non-rotating case ($\Omega = 0$), (18) becomes the same condition as that given by Wu (1987) and Lepeltier & Aly (1996) who considered non-rotating current sheets. The condition (16) becomes that given by Anzer (1969) and Spruit & Taam (1990) provided one sets $\Omega_K = 0$. This is because these authors omitted gravitational restoring forces in the direction perpendicular to the current sheet.

The local criterion for stability becomes satisfied when the disc is being primarily supported by an external field. For an external dipole

$$\frac{r}{B_z} \frac{\partial B_z}{\partial r} = -3.$$

Then (18) will be satisfied when the magnetic field provides enough support against gravity so that $\Omega_K^2 > 3\Omega^2/2$. The latter is satisfied in the interior regions of the disc where the field lines link to the central dipole and Ω is constant with Ω_K increasing inwards.

We note that the condition above has been obtained for small $|k|$, which is out of the domain of validity of a local approximation. However, the term in (15) involving $|k|$ is proportional to $(B_r^+)^2$ and it therefore becomes of decreasing importance for a uniformly rotating magnetically supported region as this extends inwards towards regions of large B_z , with the result that instability must eventually ensue. However, the precise details of onset require explicit calculation.

3.3 Axisymmetric Modes

Rigorous global criteria may be obtained in the case of axisymmetric modes through the existence of variational principles. In this case, for $m = 0$, (14) can be written in the form

$$\sigma^2 \xi_z = \mathcal{O}(\xi_z), \quad (19)$$

where the operator \mathcal{O} is self-adjoint in that for arbitrary eigenfunctions ξ_z and η_z the following equality is satisfied

$$\int_{R_i}^{R_o} \Sigma r \eta_z^* \mathcal{O}(\xi_z) dr = \left(\int_{R_i}^{R_o} \Sigma r \xi_z^* \mathcal{O}(\eta_z) dr \right)^*.$$

In this case, a sufficient condition for instability is that, for any ξ_z ,

$$\begin{aligned} \int_{R_i}^{R_o} \Sigma r \xi_z^* \mathcal{O}(\xi_z) dr &= \int_{R_i}^{R_o} \Sigma r \left(\Omega_K^2 + \frac{2B_r^+}{\Sigma} \frac{\partial B_z}{\partial r} \right) |\xi_z|^2 dr \\ &+ \frac{1}{\pi} \int_{R_i}^{R_o} \int_{R_i}^{R_o} \int_0^{2\pi} \frac{(B_z^+(r))^* B_z^+(r') \cos(m\varphi') r r' dr dr' d\varphi'}{\sqrt{r'^2 + r^2 - 2r r' \cos(\varphi')}} < 0. \end{aligned} \quad (20)$$

On insertion of suitable local trial functions, this gives the same condition as (15).

3.4 Relation to thick disc analysis

We here note that the above variational principle may also be derived from the general variational principle of Papaloizou & Szuszkiewicz (1992) for stability to adiabatic perturbations of a general differentially rotating equilibrium with a purely poloidal magnetic field, when the thin disc limit is taken.

This establishes that the results are not an artefact of the use of the razor-thin disc approximation and vertically averaged equations from the outset. A sufficient condition for stability to axisymmetric modes is that for any trial ξ :

$$\int \xi^* \cdot \mathbf{L}(\xi) dV < 0 \quad (21)$$

where \mathbf{L} is a linear operator, defined in Papaloizou & Szuszkiewicz (1992) and below, similar in principle to \mathcal{O} but which depends on both r and z . The integral is now a volume integral (see below).

The condition (21) is also necessary for stability to density perturbations with odd symmetry with respect to reflection in the equatorial plane such that $(\xi_r, \xi_\varphi, \xi_z) \rightarrow (-\xi_r, -\xi_\varphi, \xi_z)$. This corresponds to modes of the symmetry type considered in this paper. For these we have instability if

$$- \int \xi^* \cdot \mathbf{L}(\xi) dV = \int \left(\frac{|P'|^2}{\Gamma_1 P} + \rho Q(\xi, \xi^*) - \frac{j_\varphi}{r} (\xi \cdot \nabla(\psi')^* + \xi^* \cdot \nabla\psi') + \frac{|\nabla\psi'|^2}{r^2} \right) dV < 0. \quad (22)$$

Here, ρ , Γ_1 and ψ' denote the density, specific heat ratio and magnetic flux perturbation respectively. For a fluid with smoothly vanishing density and pressure at the boundary all integrals, other than the last, are taken over the fluid volume V . The last integral which is related to the magnetic energy associated with the perturbation must be taken over the whole of space excluding any perfect conductors. The pressure perturbation is given by

$$P' = -\Gamma_1 P \nabla \cdot \xi - \xi \cdot \nabla P.$$

The quadratic form $Q(\xi, \xi^*)$ is given by

$$Q(\xi, \xi^*) = r(\xi^* \cdot \nabla r)(\xi \cdot \nabla \Omega^2) - \xi^* \cdot \frac{\nabla P}{\rho} \xi \cdot \left(\frac{\nabla P}{\Gamma_1 P} - \frac{\nabla \rho}{\rho} \right) - (\psi')^* \xi \cdot \nabla \left(\frac{j_\varphi}{r \rho} \right). \quad (23)$$

In our case we adopt $\xi = (0, 0, \xi_z)$ with ξ_z being real and depending only on r . For this trial function, use of $\psi' = -\xi \cdot \nabla \psi$ inside the ideal fluid, together with vertical hydrostatic equilibrium, gives

$$-\int \boldsymbol{\xi}^* \cdot \mathbf{L}(\boldsymbol{\xi}) dV = \int \left(\rho \frac{\partial^2 \Phi}{\partial z^2} + \frac{\partial B_z}{\partial r} \frac{\partial B_r}{\partial z} \right) \xi_z^2 dV + \int \frac{1}{r^2} \left(\frac{\partial}{\partial r} (\xi_z r B_r) \right)^2 dV + \int_{\text{vac}} B'^2 dV. \quad (24)$$

Here all integrals except the last are taken over the fluid disc while the last is taken over the vacuum outside.

We see that there is a close correspondence between (24) and (20) which applies to the razor-thin disc. Each of the integrals in (24) apart from the second, which becomes vanishingly small compared to the first in the thin disc limit, approaches the corresponding integral in (20). Thus the instabilities we find are not due to the *ab initio* assumption of a razor-thin disc.

3.5 A simple picture of the instability

Here we show how the condition for instability (16) can be found from a simple argument relating to the interaction of a current loop with the central dipole. For the dipole field interior to the loop to be of the same orientation as the field produced by the loop itself (no X-point), the dipole moment must have the opposite sign to the azimuthal current density which produces an unstable interaction. A current loop at (r, z) with total current I produces a magnetic field at the origin with a vertical component

$$B_0 = \frac{I r^2}{2(z^2 + r^2)^{3/2}}. \quad (25)$$

The energy of an anti-aligned dipole of dipole moment μ situated at the centre of the loop is

$$W = \mu B_0 = \frac{\mu I r^2}{2(z^2 + r^2)^{3/2}}.$$

If we suppose that the loop lies initially at $z = 0$, and that is then displaced vertically up to z , where z is small compared to r , the change on the energy is

$$\delta W = -\frac{3\mu I z^2}{4r^3}.$$

To obtain the total change in energy we must add the change in gravitational potential energy $m_s \Omega_K^2 z^2 / 2$, where m_s is the loop mass. Writing $m_s = 2\pi \Sigma r dr$, and $I = J dr$, we obtain for the total energy change

$$\delta W = \left(-\frac{3\mu J}{4\pi \Sigma r^4} + \Omega_K^2 \right) \pi \Sigma r z^2 dr.$$

Using (2) and the expression for the external vertical field produced by the dipole, $B_z^{\text{ext}} = \mu / (4\pi r^3)$, we obtain

$$\delta W = \left(\frac{2B_r^+}{\Sigma} \frac{\partial B_z^{\text{ext}}}{\partial r} + \Omega_K^2 \right) \pi \Sigma r z^2 dr.$$

The natural condition for instability is that energy be released on making the displacement, or in our case $\delta W < 0$. This gives the same condition as (16) if we replace B_z with the external vertical field which is the one that dominates under conditions of strong magnetic support.

Thus we see that the generic instability can be understood in terms of an unstable interaction between the disc current and the central dipole. In the simple example described above, when the system passes through marginal stability because of say an increasing dipole moment, a bifurcation occurs such that there is a new stable equilibrium for the current loop lying off the original mid-plane. This suggests that in the case of a continuous disc, a warped structure may be taken-up in which the inner regions are elevated above or below the symmetry plane, facilitating eventual motion towards the central object along field lines. We now go on to discuss numerical calculations of normal modes for some specific models.

4 NUMERICAL CALCULATIONS

4.1 Equilibrium disc current and flux function

In order to solve (14) we need to specify functional forms for Σ and J . The radial and vertical components of the magnetic field are then determined from ψ which is calculated using (4). To evaluate the integral in the right hand side of (4) we use the method outlined in Lubow et al. (1994). The region between R_i and R_o is divided into N_r equally spaced grid points with separation dr . The surface current density J is discretised in the form of concentric ring currents $I(r_i) = J(r_i) dr$ where subscripts i (and j later) denote values calculated at the i^{th} (j^{th}) grid point. Equation (4) is then approximated by

$$\psi(r_i) = \frac{1}{4\pi} r_i \sum_j K_{ij} I(r_j) r_j \quad (26)$$

where K_{ij} is the discretised form of the integral with respect to φ in (4); this can be written in terms of elliptic integrals (see Jackson 1975). We thus write

$$K_{ij} = \frac{4}{\sqrt{r_i^2 + r_j^2 + 2r_i r_j}} \frac{[(2 - k^2)E_1(k^2) - 2E_2(k^2)]}{k^2}$$

where $E_1(k^2)$ and $E_2(k^2)$ are elliptic integrals of the first and second kind respectively, and

$$k^2 = \frac{4r_i r_j}{r_i^2 + r_j^2 + 2r_i r_j}$$

In the numerical calculations performed here, the surface current density J is, to within a scaling factor, taken to be given by

$$J = f_J(r_i) - f_J(R_o + dr)$$

where

$$f_J(r_i) = c_1 \sqrt{4\pi} [\exp(c_2 \cdot nc(r_i - r_{\text{mid}})^2/R_o^2) + (r_i/R_o)^{c_3 \cdot nc} - 1]^{-1/nc}. \quad (27)$$

Both J and Σ can be taken to vanish at some point simultaneously in the same manner so as to retain a finite Lorentz force. We have chosen this point to be at a fictitious additional grid point at $R = R_o + dr$ for numerical convenience.

The values of the constants $c_1 \dots c_3$, r_{mid} and nc are :

$$\begin{aligned} c_1 &= 10 & c_2 &= 0.1 & c_3 &= 2 \\ nc &= 4 & r_{\text{mid}} &= 0.9R_o \end{aligned}$$

The radial distribution of ψ is calculated from equation (26). The corresponding field lines in the z^+ quarter of the disc are the contours of $\psi(r, z) = \text{const}$. To the above internally produced magnetic flux we add a contribution from a dipole at the origin given by (5). Since the disc is thin, we shall neglect the radial magnetic field produced by this dipole and consider only the vertical component.

4.2 Dimensionless variables

We define a modified epicyclic frequency κ_m such that

$$\kappa_m^2 = \Omega_K^2 + \frac{2B_r^+}{\Sigma} \frac{\partial B_z}{\partial r} \quad (28)$$

and consider the dimensionless variables $x = r/R_o$, $\bar{\kappa} = \kappa_m/\Omega_0$, $\bar{\sigma} = \sigma/\Omega_0$, $\bar{\Omega} = \Omega/\Omega_0$, $\bar{B}_r^+ = B_r^+/B_0$, $\bar{\psi} = \psi/(B_0 R_o^2)$ and $\bar{\Sigma} = \Sigma/\Sigma_0$, with $\Omega_0 = \Omega_K(R_o)$ and B_0 and Σ_0 being some fiducial values of the magnetic field and surface mass density respectively. The normal mode equation (14) can then be written in the dimensionless form

$$\left(\bar{\kappa}^2 - (\bar{\sigma} + m\bar{\Omega})^2 \right) \xi_z = -\beta_0 \frac{2\bar{B}_r^+}{\bar{\Sigma}} \frac{\partial \bar{\Phi}'_M}{\partial x} \quad (29)$$

where $\bar{\Phi}'_M = \Phi'_M/(B_0 R_o)$ and β_0 is a constant which measures the relative strength of the magnetic and centrifugal forces (the larger β_0 , the larger the magnetic support):

$$\beta_0 = \frac{B_0^2 R_o^2}{GM\Sigma_0}.$$

The dimensionless external magnetic flux in the disc ($z = 0$) takes the form $\bar{\psi}_{\text{ext}} = -\bar{\psi}_0/x$. Equilibrium models which have scaled specified profiles for disc current and surface density are parametrised by the two parameters, $\bar{\psi}_0$ which measures the ratio of dipole to disc fields and β_0 which can be thought of scaling the disc surface density to provide a desired degree of magnetic support.

In section 5 we present the results of normal mode calculations using equilibrium models with two different values of $\bar{\psi}_0$, models of type I with $\bar{\psi}_0 = 0.03$ and models of type II with $\bar{\psi}_0 = 0.06$. Various values of β_0 have been considered. We plot the dimensionless components of the magnetic field produced by the disc currents in Fig. 1. The magnitudes of the dipole field at the innermost radius are given for models of type I and II for comparison. The contours defined by $\bar{\psi}_{\text{ext}} + \bar{\psi} = \text{const}$ are plotted in Fig. 2(a) for models of type I and in Fig. 2(b) for models of type II.

4.3 Surface density and Angular velocity

The surface density and angular velocity are calculated in the following way. The magnetic support, s_m , is defined as the ratio of magnetic to centrifugal forces in the condition for radial equilibrium:

$$|s_m| = \frac{2|\bar{B}_r^+ \bar{B}_z| x^2}{\bar{\Sigma}}$$

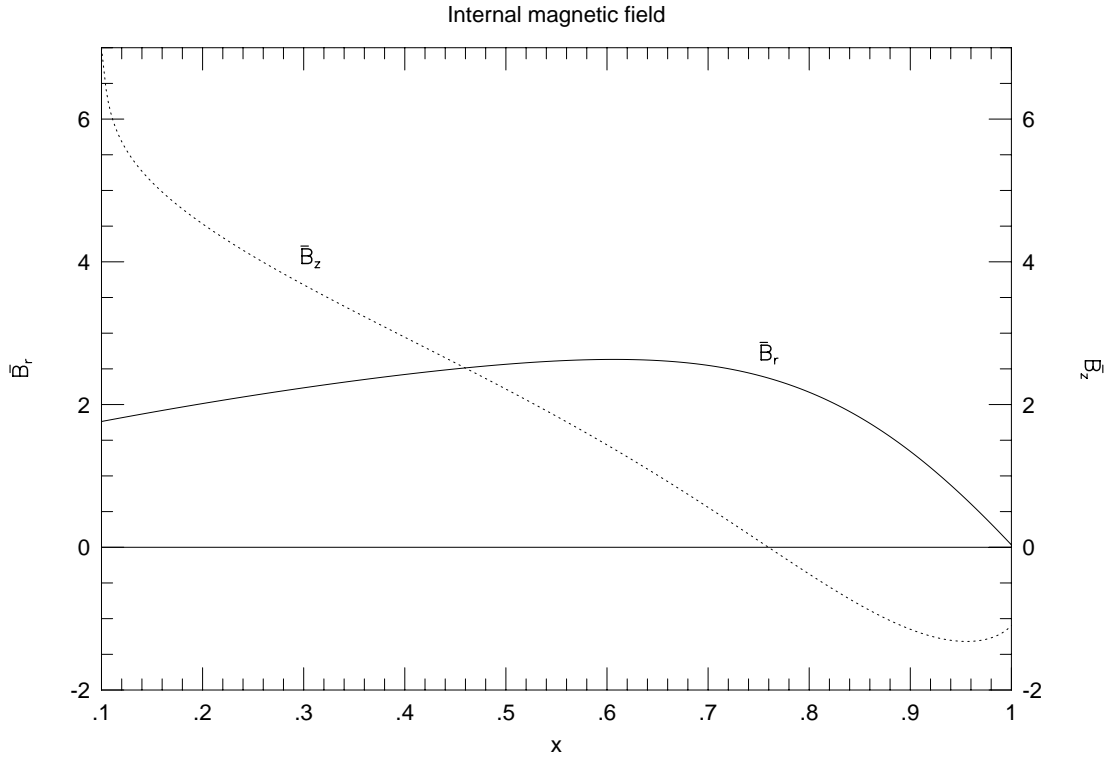


Figure 1. Radial (\bar{B}_r) and vertical (\bar{B}_z) components of the magnetic field due to the disc currents. The magnitude of the dimensionless dipole field at the centre is 30 for models of type I and 60 for models of type II

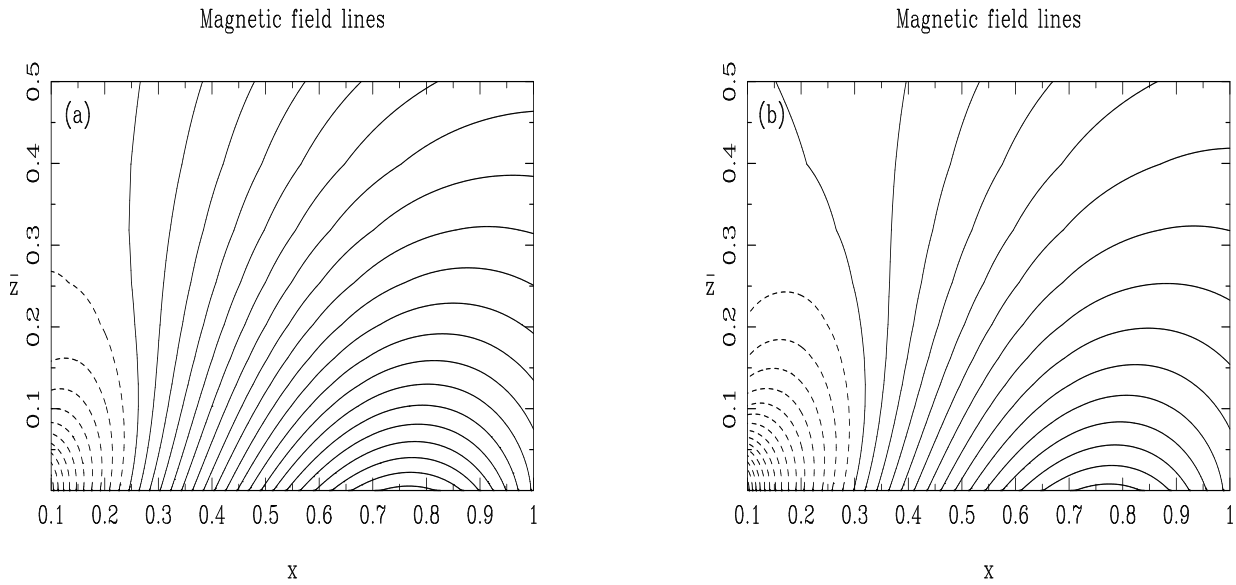


Figure 2. Magnetic field lines for (a) models of type I and (b) models of type II.

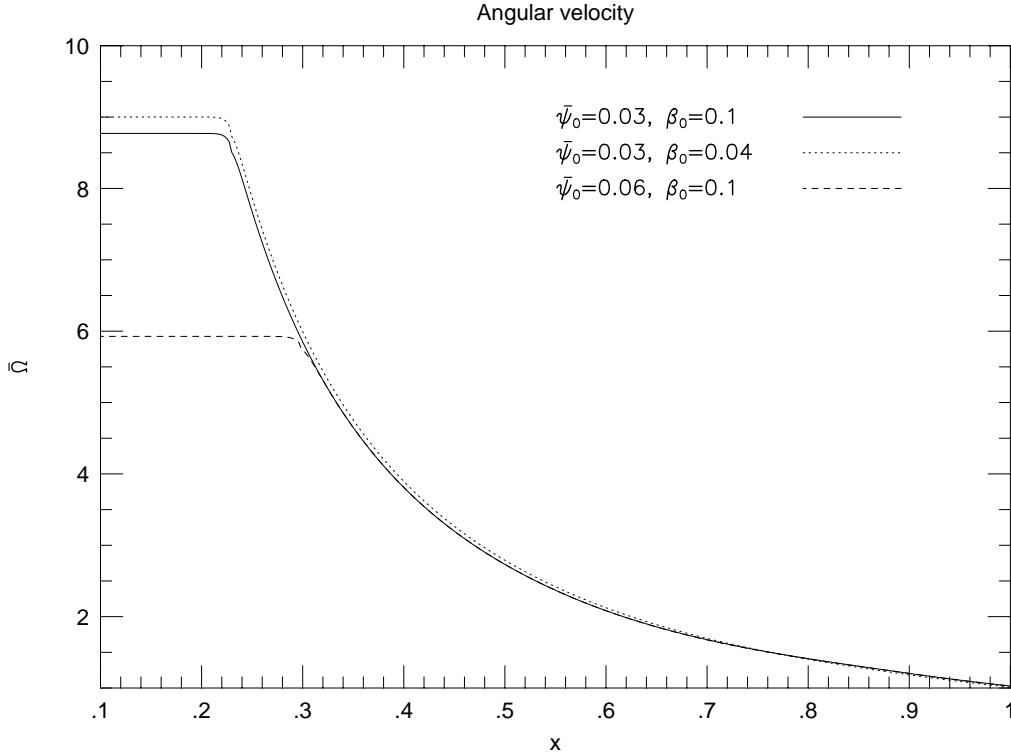


Figure 3. Angular velocity $\bar{\Omega}$ for $\bar{\psi}_0 = 0.03$ and $\beta_0 = 0.1$ (solid line), $\bar{\psi}_0 = 0.03$ and $\beta_0 = 0.04$ (dotted line) and $\bar{\psi}_0 = 0.06$ and $\beta_0 = 0.1$ (dashed line).

where $\bar{B}_z = B_z/B_0$. We first fix the value of $|s_m|$. It is reasonable to assume that in an accretion disc the magnetic support due to the internal field is larger in the inner parts of the disc than in the outer parts. This is indeed the case if the magnetic field in the disc is advected radially due to the accretion (Lubow et al. 1994, Reyez-Ruiz & Stepinski 1996, Agapitou & Papaloizou 1996). In addition, the dipole increases the magnetic support in the central region of the disc. For these reasons we take $|s_m|$ to be a decreasing function of x . $\bar{\Sigma}$ is then calculated from $|s_m|$ and adjusted in order to make sense physically. $\bar{\Omega}$ is then deduced from the dimensionless form of the radial equilibrium (3)

$$\bar{\Omega}^2 = \bar{\Omega}_K^2 - \beta_0 \frac{s_m}{x^3}, \quad (30)$$

where (2) has also been used. As mentioned above (section 2.1), the inner parts of the disc where the magnetic field lines are linked to the dipole corotate with the dipole. The dipole flux is negative whereas the disc internal flux is positive. In the inner parts of the disc the total flux is then negative and in the absence of singular points the field lines are connected to the dipole. In contrast the total flux in the outer parts of the disc is positive and the field lines are not linked to the dipole. We then fix the angular velocity $\bar{\Omega}$ to be constant in the part of the disc where the total flux is negative, equal to its value at the point where the flux vanishes. Given this new $\bar{\Omega}$ profile, we then recalculate $\bar{\Sigma}$ using (30).

We have performed calculations for disc models with a magnetic field configuration of the type described above. For all the models the inner disc radius $x_{\text{in}} = 0.1$ and the outer disc boundary is at $x_o = 1$. Figures 3 to 6 show respectively the equilibrium profiles of $\bar{\Omega}$, $\bar{\Sigma}$, s_m and $\bar{\kappa}^2$ used for models of type I and II with $\beta_0 = 0.1$ or 0.04.

From Fig. 5 we see that the inner parts of the disc are dominated by the dipole field. Indeed β_0 , which controls the strength of the disc magnetic field, does not affect the magnetic support close to the inner edge of the disc.

5 NORMAL MODE CALCULATIONS

We have performed global normal mode calculations for the disc models described above. Both axisymmetric modes and modes with small values of m have been considered and unstable spectra found.

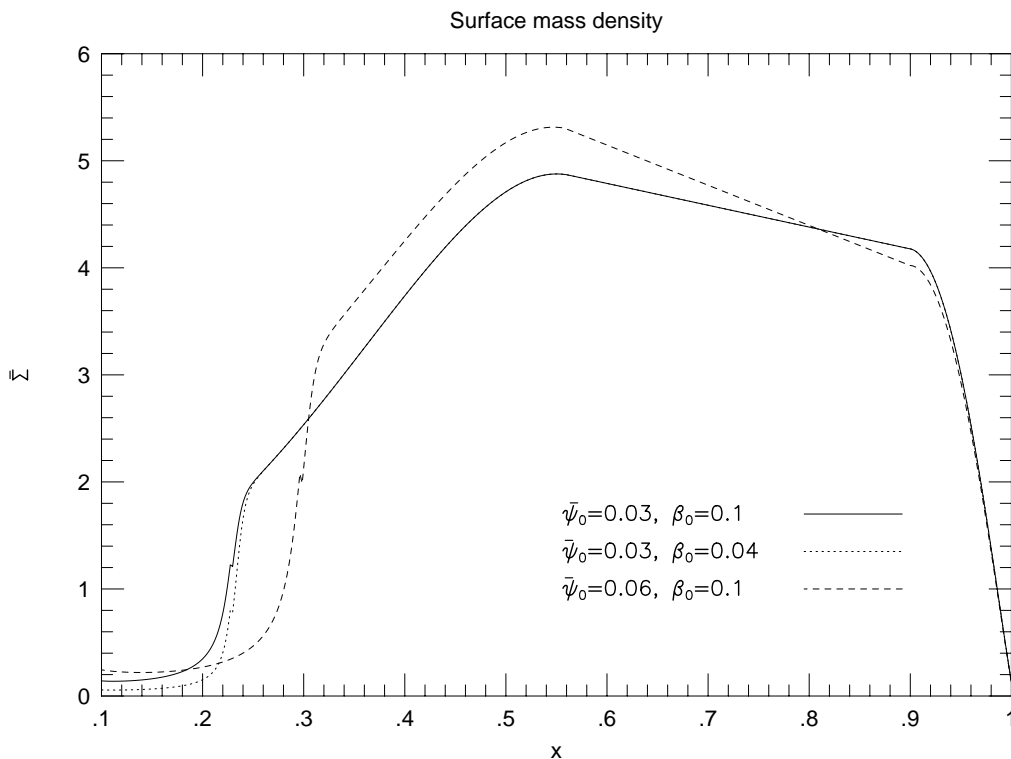


Figure 4. Surface density $\bar{\Sigma}$ for $\bar{\psi}_0 = 0.03$ and $\beta_0 = 0.1$ (solid line), $\bar{\psi}_0 = 0.03$ and $\beta_0 = 0.04$ (dotted line) and $\bar{\psi}_0 = 0.06$ and $\beta_0 = 0.1$ (dashed line).

We solve equation (29) by dividing the radial interval $[x_{\text{in}}, x_o]$ into a grid of n_r points at positions $(x_i)_{i=1 \dots n_r}$ with a spacing $\Delta x_i = x_{i+1} - x_i$. The disc boundaries are at $x_1 = x_{\text{in}} = 0.1$ and $x_{n_r} = x_o = 1$.

We approximate the integral in the expression (9) for Φ'_M by a sum of functional values at the points $(x_i)_{i=1 \dots n_r}$. Since the integrand involves ξ_z through $B_z^{'+}$ (see (7)), the discretised form of equation (29) is a system of n_r equations of the form

$$\left[(\bar{\sigma} + m\bar{\Omega}_i)^2 - \bar{\kappa}_i^2 \right] \xi_{z,i} = \sum_{j=1}^{n_r} A_{ij} \xi_{z,j}, \quad i = 1 \dots n_r \quad (31)$$

where the subscript i (or j) denotes the value of the function at the point x_i (or x_j) and A is a matrix which depends on the characteristics of the disc. If $m = 0$, (31) is a $n_r \times n_r$ eigensystem with eigenvalue $\bar{\sigma}$ and eigenfunctions $\xi_{z,i}, i = 1 \dots n_r$. For m non-zero, we set

$$u_i = \frac{\bar{\sigma}}{2m\bar{\Omega}_i} \xi_{z,i}.$$

The system (31) is then equivalent to a $2n_r \times 2n_r$ eigensystem with eigenvalue $\bar{\sigma}$ and eigenfunctions $\xi_{z,i}, i = 1 \dots n_r$ and $u_i, i = 1 \dots n_r$. The eigenvalues are calculated numerically using the QR algorithm for real Hessenberg matrices given by Press et al. (1986). Once $\bar{\sigma}$ is found, the solution of the system (31) gives $\xi_{z,i}, i = 1 \dots n_r$.

Table 1 summarises the characteristics of the disc models considered. For a mode to be unstable we require that $\text{Im}(\bar{\sigma}) < 0$. The table also gives for each model the eigenvalues $\bar{\sigma}$ for the unstable modes found. The real part of $\bar{\sigma}$ is the frequency of the mode and the imaginary part relates to its growth rate. In the column which contains n_r , we have indicated whether the grid is uniform (u) or non-uniform (n).

The grids corresponding to $n_r = 864, 1175$ and 1301 are non-uniform. They are characterised by a step Δx_1 between $x = 0.1$ and 0.3 , Δx_2 between $x = 0.3$ and 0.8 , and Δx_3 between $x = 0.8$ and 1 . The values of $\Delta x_1, \Delta x_2$ and Δx_3 are given in table 2 where $\Delta x_0 = 0.9/399$.

We performed a test for model I2a by setting $\psi_{\text{ext}} = 0$. In this case with no external field, we confirmed that the disc has a zero frequency rigid tilt mode ($\xi_z \propto r$) which is the mode having the lowest frequency. When an external field is added, the

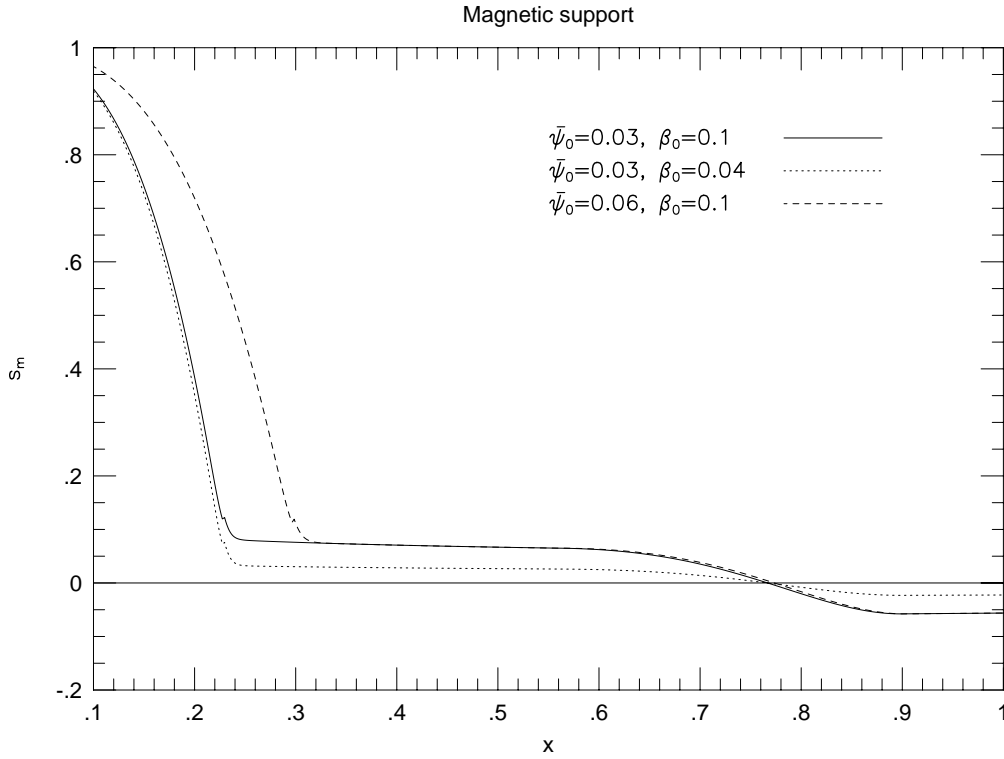


Figure 5. Magnetic support s_m for $\bar{\psi}_0 = 0.03$ and $\beta_0 = 0.1$ (solid line), $\bar{\psi}_0 = 0.03$ and $\beta_0 = 0.04$ (dotted line) and $\bar{\psi}_0 = 0.06$ and $\beta_0 = 0.1$ (dashed line).

Table 1. Characteristics of the disc models and values of $\bar{\sigma}$ for unstable modes.

Model	$\bar{\psi}_0$	β_0	m	n_r	$\bar{\sigma}$ (the unresolved modes are followed by *)
I1	0.03	0.1	0	799 (u)	(0,-37.44) (0,-17.31) (0,-7.62)
I2a	—	—	1	799 (u)	(-8.77,-37.22) (-8.77,-17.80) (-8.77,-7.31)
I2b	—	—	—	1175 (n)	(-8.79,-36.90) (-8.79,-17.47) (-8.79,-6.72)
I3a	—	—	2	799 (u)	(-17.54,-37.16) (-17.54,-18.21) (-17.54,-7.41)
I3b	—	—	—	864 (n)	(-5.07,-0.0013)* (-4.49,-0.0015)* (-4.02,-0.0032)* (-17.54,-37.14) (-17.54,-18.20) (-17.54,-7.40) (-6.78,-0.0008)*
I4a	—	—	3	864 (n)	(-26.31,-37.13) (-26.31,-18.60) (-26.31,-7.70)
I4b	—	—	—	1301 (n)	(-17.16,-0.0029)* (-7.70,-0.0019)* (-5.83,-0.0035)* (-5.39,-0.0019) (-26.31,-37.13) (-26.31,-18.60) (-26.31,-7.70)
I5	—	0.04	1	799 (u)	(-11.26,-0.0013)* (-9.17,-0.0012)* (-6.53,-0.0026)* (-6.30,-0.0022)* (-5.83,-0.0024)* (-5.40,-0.0037)
II	0.06	0.1	1	799 (u)	(-9.00,-37.07) (-9.00,-17.60) (-9.00,-6.88) (-5.93,-40.33) (-5.93,-28.16) (-5.93,-23.06) (-5.93,-17.41) (-5.93,-12.95) (-5.93,-6.91)

Table 2. Characteristics of the non uniform grids

n_r	Δx_1	Δx_2	Δx_3
864	$\Delta x_0/2$	Δx_0	$\Delta x_0/4$
1175	$\Delta x_0/8$	$\Delta x_0/2$	$\Delta x_0/2$
1301	$\Delta x_0/2$	Δx_0	$\Delta x_0/8$

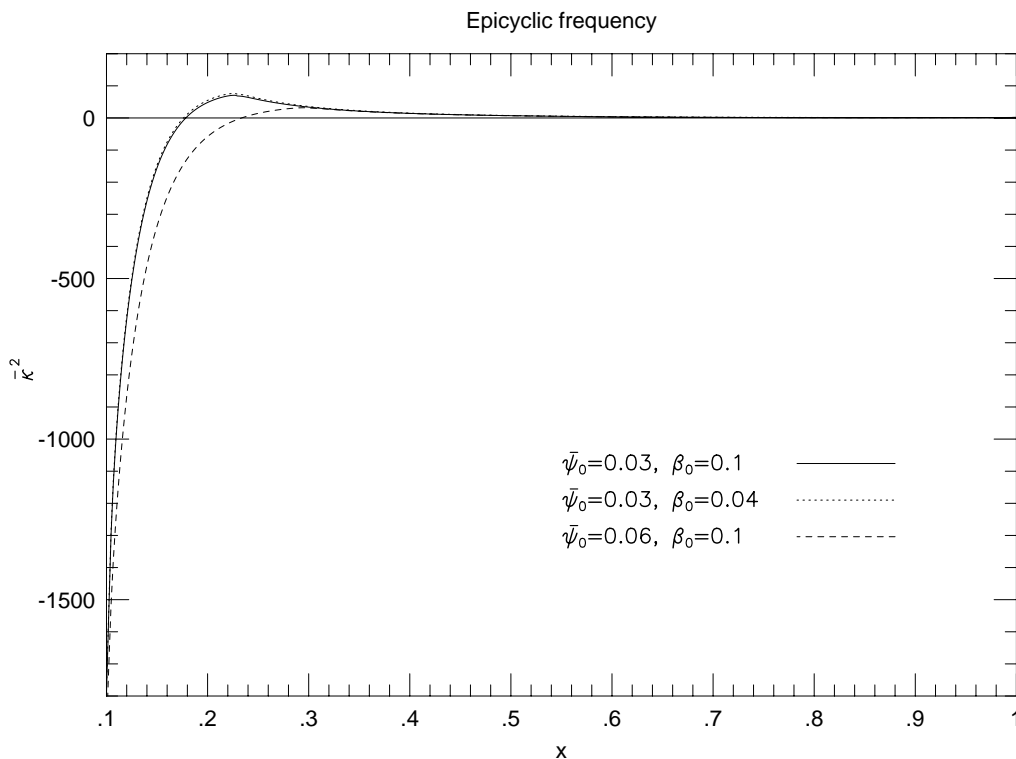


Figure 6. Square of the epicyclic frequency, $\bar{\kappa}^2$, for $\bar{\psi}_0 = 0.03$ and $\beta_0 = 0.1$ (solid line), $\bar{\psi}_0 = 0.03$ and $\beta_0 = 0.04$ (dotted line) and $\bar{\psi}_0 = 0.06$ and $\beta_0 = 0.1$ (dashed line).

equivalent mode is a modified rigid tilt mode, as shown on Fig. 7. Since the dipole field is significant only in the inner parts of the disc, this mode takes on the character of a rigid tilt mode in the outer parts.

For $m = 0$ and $m = 1$, all the unstable modes are well resolved. For higher values of m , in addition to well resolved unstable modes we get some poorly resolved weakly unstable ones. The number, frequency and growth rate of these modes depend on the grid resolution. However, in all cases they have growth rates several orders of magnitude smaller than those of the well resolved modes. Thus, although their reality is questionable, they are not important, and from now on we shall consider only the spectrum consisting of the well resolved unstable modes.

These modes are confined in the inner parts of the disc where $\bar{\kappa}^2 < 0$ (see Fig. 6). This is in agreement with the local dispersion relation which predicts that instability ensues when the condition (16) is satisfied. The frequency of these modes is $-m\bar{\Omega}_c$, where $\bar{\Omega}_c$ is the angular velocity in the inner parts of the disc, and their growth rate depends only weakly on m . For each m , the most unstable modes have a growth rate significantly larger than their frequency indicating dynamical instability. The number of modes in the unstable spectrum increases with the strength of the magnetic support in the inner parts of the disc, as does the growth rate of the most unstable mode.

For $\bar{\psi}_0 = 0.03$ there are 3 unstable modes, with respectively 0, 1 and 2 nodes in the real part of ξ_z , whereas for $\bar{\psi}_0 = 0.06$ there are 6 modes, with the number of nodes varying between 0 and 5 (the smaller the growth rate, the larger the number of nodes). Fig. 8 and Fig. 9 show the real part of ξ_z in the inner parts of the disc for models I2a and II respectively. In all cases the imaginary part of ξ_z is very small compared to its real part. We note that the characteristics of these modes do not depend on the resolution.

Varying β_0 hardly changes the characteristics of the unstable modes. As mentioned above, the inner parts of the disc, where the modes are confined, are indeed dominated by the dipole field where conditions are insensitive to β_0 .

In the equilibrium models to which the above calculations correspond, the internal vertical field vanishes at some location in the outer parts of the disc. To check whether the results depend on the unlikely presence of this O-point, we have re-run model I2a and model I3 with $n_r = 1301$ and the outer boundary at $x = 0.7$. The results are very similar to those obtained above, the minor differences coming from the fact that the rotation and the density profiles are a bit different in the two

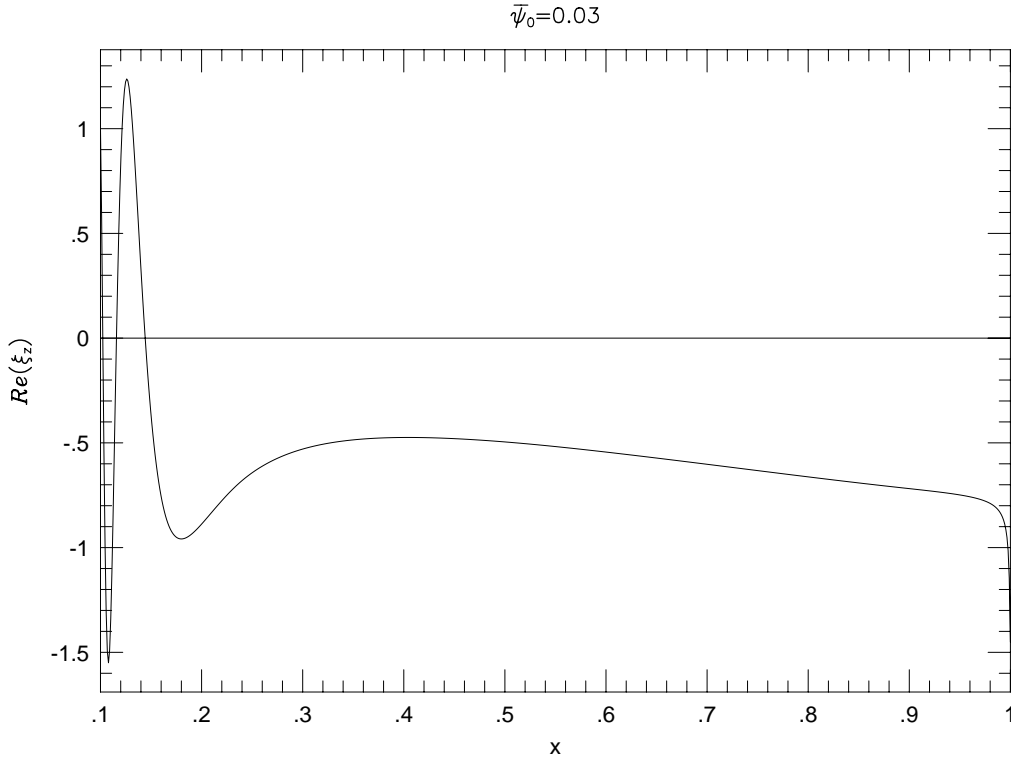


Figure 7. $\text{Re}(\xi_z)$ for $\bar{\psi}_0 = 0.03$, $\beta_0 = 0.1$, $m = 1$ and $n_r = 799$ (model I2a). The mode represented is the modified rigid tilt mode and has $\bar{\sigma} = (-0.025, 0)$.

cases. This is consistent with the fact that the internally confined unstable modes are almost independent of the structure of the outer parts of the disc.

6 DISCUSSION

In this paper, we have studied the stability of a magnetized accretion disc to disturbances perpendicular to its plane (bending modes). At equilibrium, the disc is permeated by both an internally produced poloidal magnetic field and an external dipole field. The former arises from a toroidal current in the disc, the latter is supposed to originate from a magnetized central star. In the important inner regions of the disc, the field lines are in a state of isorotation. We suppose that the uniformly rotating inner disc could be produced by material diffusing inwards through the action of interchange instabilities (Spruit & Taam 1990) when the mass injection rate into the disc is high enough to enable that to occur with ultimate accretion onto and spin up of the central star. We have neglected a possible toroidal component of the magnetic field which would be produced through differential rotation if poloidal field lines connected points with different angular velocity. Since the disc is supposed to be infinitesimally thin, radial pressure gradients have been neglected.

A local stability analysis leads to the m independent condition for instability $\kappa_m^2 < 0$ (see (16)), where κ_m is the modified epicyclic frequency defined by the relation (28). In the inner regions of the disc, where the dipole field predominates over the internal one, this condition is satisfied if the magnetic field provides enough support against gravity (see (18)). We note that even though uniform rotation acts in favour of the instability, bending modes in an entirely differentially rotating disc may also be unstable. An external dipole is not absolutely necessary for instability to occur.

For axisymmetric modes, the existence of a variational principle leads to the rigorous global criterion (20) which is equivalent to (16) when local displacements are considered. Even though the razor-thin disc approximation has been used so far, the instabilities are not an *ab initio* artefact of this assumption. The criterion (20) is the thin disc limit of the general variational principle of Papaloizou & Szuszkiewicz (1992) for axisymmetric modes.

We have solved numerically the normal mode equation (14) for specific disc equilibrium models. For low values of m we get a

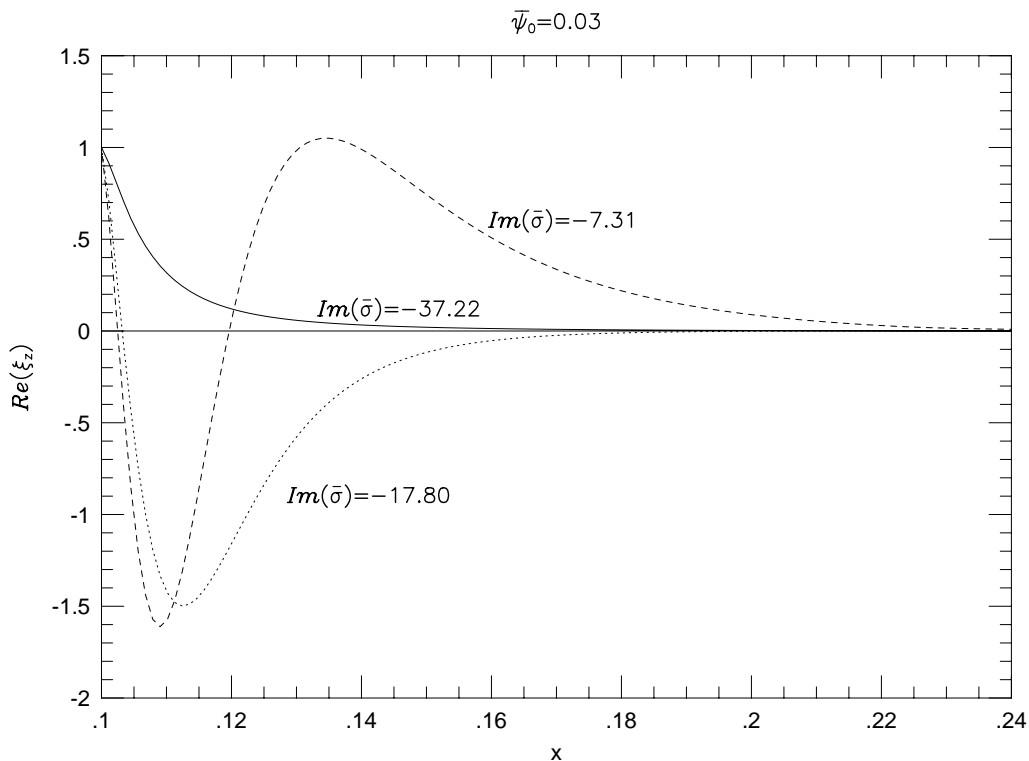


Figure 8. $\text{Re}(\xi_z)$ for $\bar{\psi}_0 = 0.03$, $\beta_0 = 0.1$, $m = 1$ and $n_r = 799$ (model I2a). The modes represented have $\text{Re}(\bar{\sigma}) = -8.77$ and $\text{Im}(\bar{\sigma}) = -37.22$ (solid line), $\text{Im}(\bar{\sigma}) = -17.80$ (dotted line) and $\text{Im}(\bar{\sigma}) = -7.31$ (dashed line). Only the inner parts of the disc are represented.

spectrum of well resolved dynamically unstable modes, which are confined in the inner parts of the disc where $\kappa_m^2 < 0$. For a given m , the number N of these modes increases with the magnetic support. For these the tendency is that the number of nodes in the real part of the vertical displacement increases from 0 to $N - 1$. This is similar to what happens in a non-magnetized, self-gravitating, uniformly rotating disc (we have already mentioned in section 3.2 the similarity between the two situations). In that case, Hunter & Toomre (1969) have indeed shown that the normal modes of free oscillation are polynomials with increasing numbers of nodes. However, in the self-gravitating disc, the bending modes are always stable.

We have found numerically that the pattern speed associated with the unstable modes is $\sim \Omega_c$, with Ω_c being the constant angular velocity in the inner parts of the disc.

We have argued that the instability of axisymmetric modes can be thought of as an unstable interaction between the disc current and the central dipole. Instability arises from the fact that the energy of the dipole in the magnetic field produced by the disc currents decreases due to the perturbation.

The determination of the outcome of these instabilities awaits a non-linear analysis. However, we comment that if such instabilities occur, a configuration where the inner regions of the disc are displaced from the equatorial plane of the central star may be possible. Then the accretion of the disc material along the dipole field lines will be facilitated and may occur preferentially onto one stellar hemisphere depending on the mixture of normal modes present. Non-axisymmetric instabilities may result in a quasi periodic light variation even when the disc angular momentum vector at large distances and the central dipole axis are aligned. The asymmetric magnetospheric accretion would result in an observational signature of the star-disc configuration. The periodic light variation of Classical T Tauri stars is mostly interpreted as rotational modulation of the stellar flux by hot spots due to magnetospheric accretion (see, for example, Bouvier et al. 1995). If accretion occurs preferentially to one hemisphere, then depending on the orientation of the observer the periodic light variation will be observed. The non-axisymmetric bending of the disc plane would lead to hot spots being created on the stellar surface and to the rotational modulation of the stellar output, even when the axis of the stellar dipole is aligned with the axis of rotation of the accretion disc.

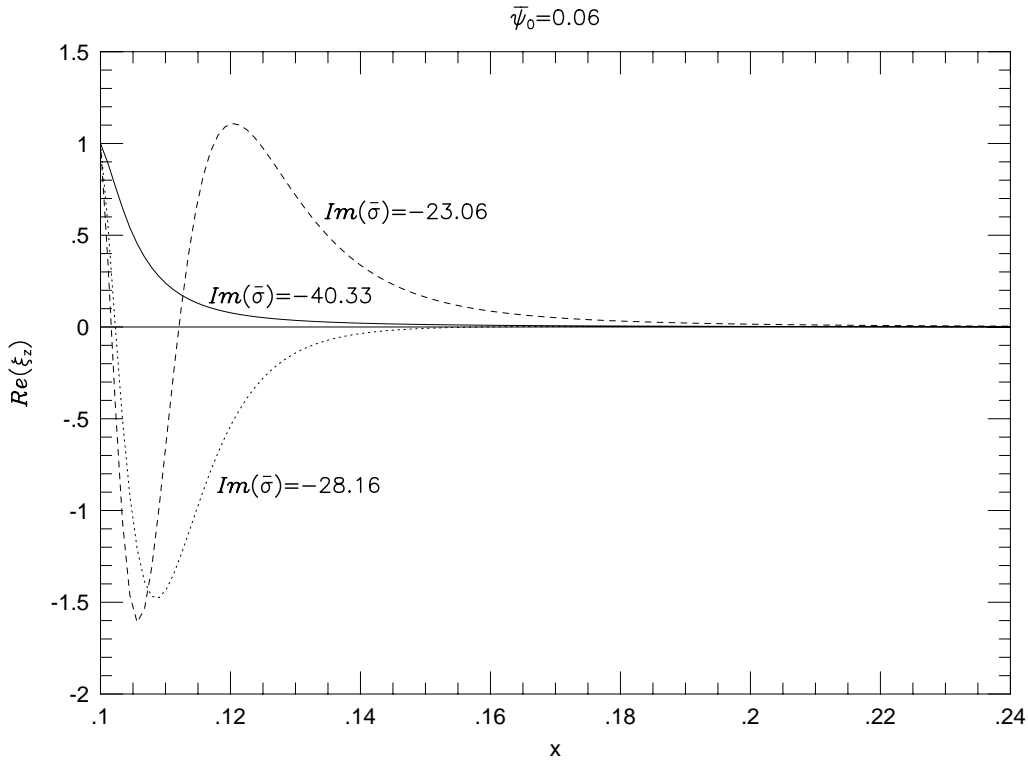


Figure 9. $\text{Re}(\xi_z)$ for $\bar{\psi}_0 = 0.06$, $\beta_0 = 0.1$, $m = 1$ and $n_r = 799$ (model II). The modes represented have $\text{Re}(\bar{\sigma}) = -5.93$ and $\text{Im}(\bar{\sigma}) = -40.33$ (solid line), $\text{Im}(\bar{\sigma}) = -28.16$ (dotted line) and $\text{Im}(\bar{\sigma}) = -23.06$ (dashed line). Only the inner parts of the disc are represented.

ACKNOWLEDGMENTS

This work was supported by PPARC grant GR/H/09454 and the EU grant ERB-CHRX-CT93-0329. C.T. acknowledges support by the Center for Star Formation Studies at NASA-Ames Research Center and the University of California at Berkeley and Santa-Cruz. V.A. acknowledges support by the State Scholarships Foundation (IKY) of the Republic of Greece through a postgraduate studentship.

REFERENCES

- Agapitou V., Papaloizou J.C.B., 1996, *Astro. Lett. & Comm.*, 34, 363
 Anzer U., 1969, *Solar Physics*, 8, 37
 Armitage P.J., Clarke C.J., 1996, *MNRAS*, 280, 458
 Bouvier J., 1994, in Caillault J.-P., ed., *Eighth Cambridge Workshop on Cool Stars, Stellar Systems and the Sun*, ASP Conference Series, vol. 64
 Bouvier J., Covino E., Kovo O., Martin E.L., Matthews J.M., Terranegra L., Beck S.C., 1995, *A&A*, 299, 89
 Brandenburg A., Tuominen I., Moss D., 1989, *Geophys. Astrophys. Fluid Dyn.*, 49, 129
 Cabrit S., Edwards S., Strom S.E., Strom K.M., 1990, *ApJ*, 354, 687
 Calvet N., Hartmann L., 1992, *ApJ*, 386, 239
 Camenzind M., 1990, *Rev. Mod. Astron.*, 3, 234
 Cameron A.C., Campbell C.G., 1993, *MNRAS*, 274, 309
 Campbell C.G., 1987, *MNRAS*, 229, 405
 Edwards S., Hartigan P., Ghandour L., Androulis C., 1994, *AJ*, 108, 1056
 Edwards S., Strom S.E., Hartigan P., Strom K.M., Hillenbrand L.A., 1993, *AJ*, 106, 372
 Ghosh P., 1995, *MNRAS*, 272, 763
 Ghosh P., Lamb F.K., 1978, *ApJ*, 223, L83
 Ghosh P., Lamb F.K., 1979, *ApJ*, 234, 296
 Hartmann L., Hewett R., Calvet N., 1994, *ApJ*, 426, 669

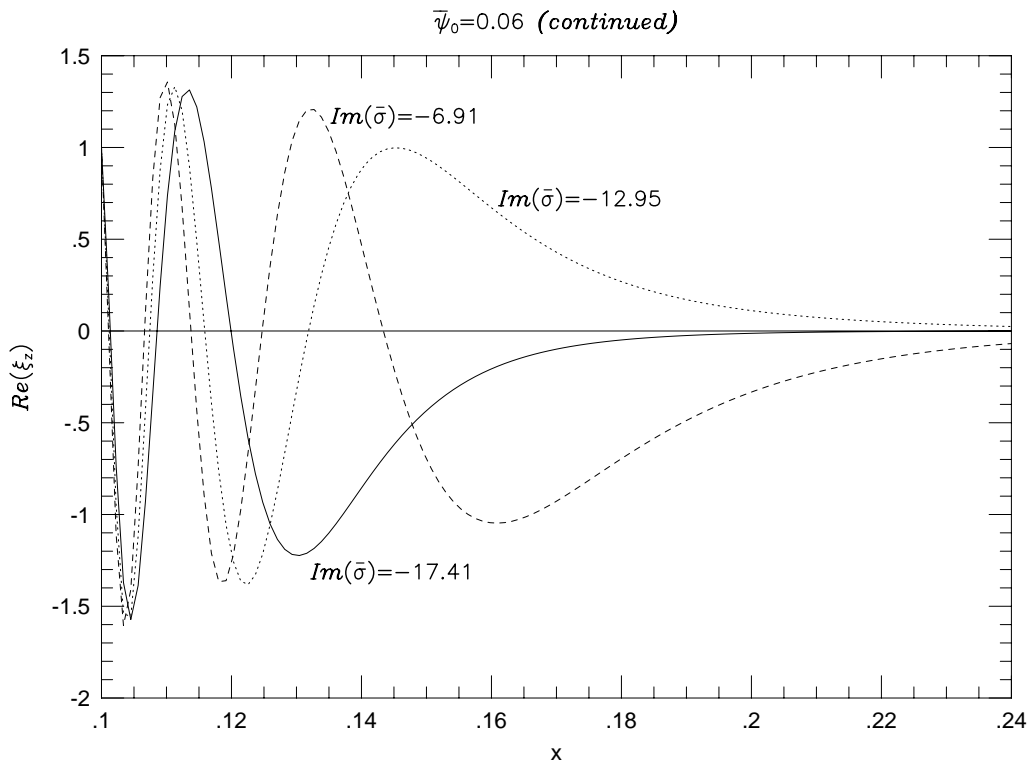


Figure 9 – *continued* The modes represented have $\text{Re}(\bar{\sigma}) = -5.93$ and $\text{Im}(\bar{\sigma}) = -17.41$ (solid line), $\text{Im}(\bar{\sigma}) = -12.95$ (dotted line) and $\text{Im}(\bar{\sigma}) = -6.91$ (dashed line).

Hunter C., Toomre A., 1969, ApJ, 155, 747

Jackson J.D., 1975, Classical Electrodynamics. Wiley, New York

Kenyon S.J., Yi I., Hartmann L., 1996, ApJ, 462,439

Königl A., 1989, ApJ, 342, 208

Königl A., 1991, ApJ, 370, L39

Königl A., 1993, in Levy E.H., Lunine J.I., eds., Protostars and Planets III. Univ. Arizona Press, Tuscon, p. 641

Lehmann T., Reipurth B., Brandner W., 1995, A&A, 300, L9

Lepeltier T., Aly J.J., 1996, A&A, 306, 645

Lubow S.H., Papaloizou J.C.B., Pringle J.E., 1994, MNRAS, 267, 235

Montmerle T., Andr'e P., Casanova S., Feigelson E.D., 1993, in Lynden-Bell D., ed., NATO Advanced Workshop on Cosmical Magnetism. Kluwer, Dordrecht

Montmerle T., Feigelson E.D., Bouvier J., Andr'e P., 1994, in Levy E.H., Lunine J.I., eds., Protostars and Planets III. Univ. Arizona Press, Tuscon, p. 689

Ogilvie G., 1997, MNRAS, 288, 63

Paatz G., Camenzind M., 1996, A&A, 308, 77

Paczynski B., 1991, ApJ, 370, 597

Papaloizou J.C.B., Lin D.N.C., 1995, ARA&A, 33, 505

Papaloizou J.C.B., Szuszkiewicz E., 1992, Geophys. Astrophys. Fluid Dyn., 66, 223

Papaloizou J.C.B., Terquem C., 1995, MNRAS, 227,553

Popham R., Narayan R., 1991, ApJ, 370, 604

Press W.H., Flannery B.P., Teukolsky S.A., Vetterling W.T., 1986, Numerical Recipes: The Art of Scientific Computing, Cambridge University Press

Reyez-Ruiz M., Stepinski T.F., 1996, ApJ, 459, 653

Shu F.H., 1984, in Greenberg R., Brahic A., eds., Planetary Rings. Univ. Arizona Press, Tuscon, p. 513

Spruit H.C., Taam R.E., 1990, A&A, 229, 475

Spruit H.C., Taam R.E., 1993, ApJ, 402, 593

Spruit H.C., Stehle R., Papaloizou J.C.B., 1995, MNRAS, 275, 1223

Tagger M., Henriksen R.N., Sygnet J.F., Pellat R., 1990, ApJ, 353, 654

Tayler R. J., 1987, MNRAS, 227, 553

Wu F., 1987, *ApJ*, 320, 418

Yi I., 1994, *ApJ*, 428, 760